Conductivity and quenched-in defects in hydrogenated amorphous silicon

Howard M. Branz,* Kenneth Capuder, Elmer H. Lyons, John S. Haggerty, and David Adler†
Massachusetts Institute of Technology, Cambridge, Massachusetts 02139
(Received 20 April 1987)

We report measurements of the electrical conductivity of hydrogenated amorphous silicon (*a*-Si:H) films prepared from laser-induced chemical-vapor deposition of silane. Intrinsic as well as *p*-type and *n*-type samples have been investigated, and the conductivity was measured after different annealing and quenching cycles. We suggest that metastable defects are introduced into the films via equilibration at high temperatures and are frozen in below a temperature that depends on thermal history. These defects result in a net movement of electronic states from below to above the Fermi level in phosphorus-doped *a*-Si:H and vice versa for boron-doped *a*-Si:H. We develop a model that is in agreement with the time dependence of the conductivity during annealing of these defects and determine that a 1.1-eV potential barrier retards equilibration.

I. INTRODUCTION

There has been a great deal of recent work indicating that thin films of glow-discharge deposited hydrogenated amorphous silicon (*a*-Si:H) reach some sort of thermal equilibration above a specific temperature, T^*, with a nonequilibrium structure frozen-in below that temperature.[1–6] The evidence for such equilibration has primarily come from electrical conductivity measurements on *n*-type[1,2] and *p*-type[3] films, from transient sweep-out measurements on *i-n-i* and *i-p-i* devices[3–5] and from subgap absorption and photoconductivity experiments on undoped films.[6] In this paper we report electrical conductivity studies of metastable defect formation and annealing processes in *a*-Si:H grown by the laser-induced chemical-vapor deposition (LICVD) technique.[7,8] These processes, which are induced by rapid cooling or heating, shift the Fermi level, E_F, and thus change the conductivity, σ, exponentially. We suggest a theory that relates changes in σ to the metastable defect density and use this theory together with our experimental data to examine the kinetics of the reequilibration processes after abrupt heating from below to above T^*. We assume that first-order relaxation of a metastable defect is responsible for the reequilibration, and obtain estimates for the concentration of defect states and for the energy barrier to equilibration. It is clear from previous experiments and from theory[9] that T^* depends on the annealing time and the cooling rate, but the experiments on LICVD *a*-Si:H demonstrate an additional, previously unobserved, dependence of T^* on the deposition technique.

II. EXPERIMENTAL TECHNIQUES

Films of *a*-Si:H were deposited by the LICVD technique, in which SiH_4 and dopant gases are pyrolized by a continuous-wave CO_2 laser beam that passes parallel to a temperature-controlled substrate. Details of the growth,[10] properties,[11] and doping[12,13] of LICVD films were presented elsewhere. Table I shows the substrate temperature (T_s), dopant type, gas-phase dopant ratio, estimated solid-phase dopant concentration, thickness, and approximate activation energy for conduction of the films studied. Each film was deposited onto Al electrodes preevaporated on a fused-silica substrate. The two 1-cm-long electrodes were 180 μm apart, so the applied voltage of 18 V corresponds to an average field strength of 10^3 V/cm. Current passing between the electrodes was measured with a Keithley 610C ammeter. The Ohmic nature of the contacts was verified, and measurements were made at pressures between 5×10^{-7} and

TABLE I. Some physical properties of investigated samples.

Sample no.	T_s (°C)	Dopant	Concentration ratio $[PH_3]/[SiH_4]$ or $[B_2H_6]/[SiH_4]$	Est. $[P/Si]$ or $[B]/[Si]$	t (μm)	E_a (eV)
243	400	P	4.4×10^{-3}	1.5×10^{-2}	0.6	0.2
245	400	P	4.4×10^{-5}	1.5×10^{-4}	0.4	0.5
246	400	P	8.8×10^{-3}	3×10^{-2}	0.9	0.2
312	300	B	2×10^{-5}	10^{-2}	0.6	0.2
230	300				0.8	0.8
332	400				0.7	0.6

2×10^{-6} Torr to minimize the importance of surface effects. During measurement, the sample rested on a metal block and the temperature was recorded by a thermocouple imbedded near the top surface of the block.

Before each measurement, samples were annealed at a temperature, T_a (typically 50 °C below its deposition temperature), for 30 to 120 min to anneal out the metastable defects not under study. The samples were then cooled to room temperature, either by quenching at a rate greater than 10 °C/sec or by controlled slow cooling at 0.01 °C/sec. Slower cooling rates were also used, but showed no significant difference from the 0.01 °C/sec results. To quench samples, we removed them from the temperature-controlled block and placed them in thermal contact with an ice-water bath. All conductivities were measured while increasing the sample temperature.

In the "slow-heating" experiments, we twice measured the conductivity as the film temperature was increased in steps of 10–20 °C back to the annealing temperature, at an average rate of 0.5 to 1.0 °C/sec. First, $\sigma^{SC}(T)$ was measured after slow cooling and on the following day, $\sigma^{Q}(T)$ was measured after quenching the sample. In the "isothermal relaxation" experiments, we quenched an n-type sample to room temperature, measured $\sigma^{Q}(T)$ during slow heating up to 140 or 160 °C, then abruptly increased the temperature to the relaxation temperature, T_r, 30 to 120 °C higher. Subsequently, we recorded the time dependence of the conductivity, $\sigma(t)$, during isothermal annealing at T_r.

III. EXPERIMENTAL RESULTS

A. Slow heating

Figure 1 shows an Arrhenius plot of the electrical conductivity during a typical pair of slow-heating runs on a heavily doped n-type LICVD a-Si:H film (sample 243). After 30 min anneals at $T_a=320$ °C the sample was first slow-cooled (SC) and later quenched (Q) to room temperature. The conductivities after each cooling, $\sigma^{Q}(T)$ and $\sigma^{SC}(T)$, were measured as the temperature was raised at an average rate of about 0.5 °C/sec. It can be seen that $\sigma^{Q}(T)\approx2\sigma^{SC}(T)$ from 20 to 120 °C. In this low-temperature regime, the conductivity activation energy after quenching ($E_a^{Q}\approx0.7$ eV) is about 0.02 eV less than that after slow cooling. Between 170 °C and 240 °C, $\sigma^{Q}(T)$ becomes constant and approaches $\sigma^{SC}(T)$. Above 240 °C, $\sigma^{Q}(T)\approx\sigma^{SC}(T)$. This qualitative behavior is reproducible and reversible. In a different pair of runs on sample 243, for example, both $\sigma^{SC}(T)$ and $\sigma^{Q}(T)$ were lower by 15% to 35% at all temperatures than in the runs pictured in Fig. 1. However, the difference $E_a^{SC}-E_a^{Q}$ and the ratio σ^{Q}/σ^{SC} were very similar, and the two curves merged at about 280 °C. In the notation of Street *et al.*[4] the point of convergence at 240 °C is called T_E, the equilibration temperature. In sample 246, also a heavily P-doped film, a qualitatively similar result was also observed: $\sigma^{Q}(T)$ leveled out between 170 °C and 240 °C, merging with $\sigma^{SC}(T)$ at about 240 °C. As a control, we made a similar pair of runs with $T_a=90$ °C and a 2 h anneal time, and we found $\sigma^{Q}(T)\approx\sigma^{SC}(T)$ from 20 °C to 90 °C.

In contrast, we found dramatically different behavior of $\sigma^{Q}(T)$ and $\sigma^{SC}(T)$ in the lightly P-doped sample 245 during identical thermal cycling. In this case, $\sigma^{Q}(T)$ is smaller than $\sigma^{SC}(T)$ below about 260 °C and they converge above that value. There is no abrupt transition in either curve; at room temperature, $\sigma^{SC}=3\sigma^{Q}$ and the curves gradually merge at higher temperature. The reproducibility of this result was not verified.

The B-doped sample was annealed for 45 min at $T_a=285$ °C before each cooling-heating cycle. Figure 2 shows the conductivity measured during one pair of runs. As with the heavily P-doped films, the quenched conductivity was more than twice the slow-cooled value below about 125 °C, but above a temperature $T_E\sim185$ °C, the film cooling rate appears to be less important. In contrast to the results on P-doped films, from T_E to T_a, $\sigma^{Q}(T)\approx1.4\sigma^{SC}(T)$. A month later, repetition of the slow-cooled run on sample 312 resulted in a closely similar curve of $\sigma^{SC}(T)$. Repetition of the quench run yielded $\sigma^{Q}(T)\approx1.6\sigma^{SC}(T)$ at low temperatures.

Measurements on the undoped samples 332 and 230 did not reveal a clear value of T_E, nor reproducible re-

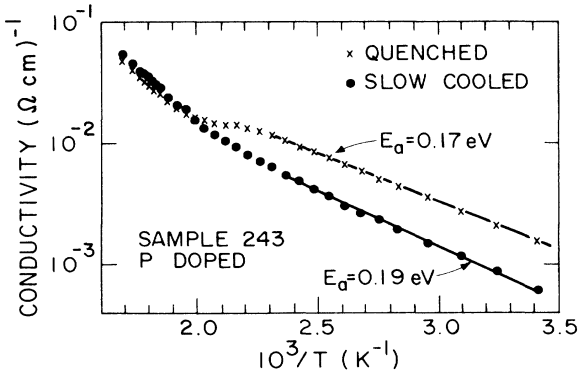

FIG. 1. Electrical conductivity vs reciprocal temperature for the n-type sample 243 after slow cooling and after quenching. Data were taken during slow heating.

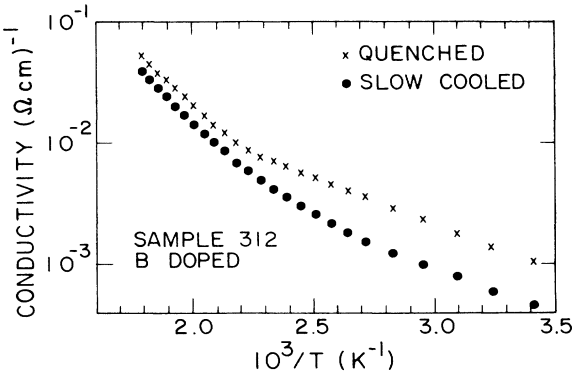

FIG. 2. Electrical conductivity vs reciprocal temperature for the p-type sample 312 after slow cooling and after quenching. Data were taken during slow heating.

sults. After 30 min anneals of sample 332 at $T_a = 90\,^{\circ}\mathrm{C}$, we found $\sigma^{Q}(T)$ and $\sigma^{SC}(T)$ were nearly identical. However, a 30-min anneal of this sample at $T_a = 320\,^{\circ}\mathrm{C}$ yielded a slow-cooled conductivity higher than the quenched conductivity at all temperatures below 300 °C. Near room temperature, $\sigma^{SC}(T)/\sigma^{Q}(T) \approx 3$, but this ratio gradually decreased as the temperature increased, reaching unity above about 300 °C. We repeated the thermal cycles and measurements after storing the sample for over 1 month at room temperature, and found $\sigma^{SC}(T) \approx \sigma^{Q}(T)$ at all temperatures, with somewhat different values of $\sigma^{SC}(T)$ and $\sigma^{Q}(T)$ compared to the earlier experiments. We measured conductivities up to $T_a = 320\,^{\circ}\mathrm{C}$ and no discernable T_E was evident in any run on sample 332. Similarly, the undoped sample 230 showed no discernable T_E below $T_a = 285\,^{\circ}\mathrm{C}$. In fact, $\sigma^{Q}(T) \approx \sigma^{SC}(T)$ below about 195 °C, but as the temperature was raised from 200 °C to 285 °C, σ^{Q} increased faster than σ^{SC}, until $\sigma^{Q} \approx 2\sigma^{SC}$ at 285 °C. The reproducibility of this result was not verified.

B. Isothermal relaxation

We performed a series of isothermal relaxation experiments by quenching the P-doped sample 243 six times after 2 h anneals at 320 °C, each time interrupting the subsequent slow heating by increasing the temperature very suddenly. The temperature jumps were from 160 °C to 280 °, 260 °C, 240 °C, 220 °C, and 200 °C or from 140 ° to 170 °C. We then annealed the sample at the higher temperature, T_r, and observed the film's relaxation by measuring $\sigma(t)$, defining $t = 0$ to be the moment that the heated block reached T_r.

In Fig. 3 we plot the ratio of the conductivity to the final conductivity, $\sigma(t)/\sigma_f$, for four values of the relaxation temperature, T_r. The film temperature lagged the heated-block temperature by 10 to 20 min, so the conductivity increased initially. After the film temperature stabilized, the conductivity decreased monotonically from its peak value, σ_{max}. While the decay is not a simple exponential, it is evident that increasing the temperature speeds the relaxation process. If we take the decay time to be the time at which $\sigma(t) - \sigma_f$ has fallen to $1/e$ of its peak value, then the decay time is roughly an activated function of T_r. A more rigorous definition of the decay time and evaluation of its dependence on T_r will be described later.

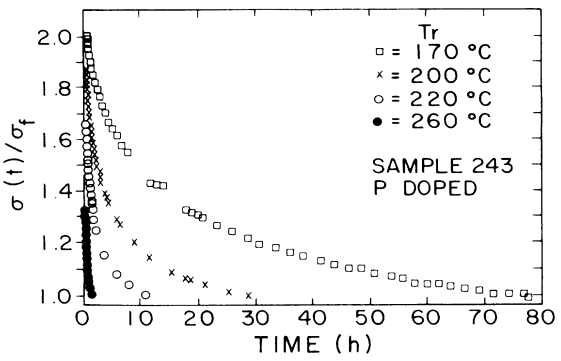

FIG. 3. Electrical conductivity of quenched sample 243 during isothermal annealing after an abrupt temperature increase.

Finally, we note that σ_{max} is not simply given by an extrapolation of $\sigma^{Q}(T)$ from low temperatures up to $\sigma^{Q}(T_r)$. For each quench and each value of T_r, $\sigma^{Q}(T_r)$ was evaluated by extrapolating to T_r the conductivities measured during slow heating from 20 °C and 160 °C. In each case, the peak value of $\sigma(t)$ is significantly higher than this extrapolated conductivity. Though this is an indirect measurement, it appears that the activation energy of $\sigma^{Q}(T)$ increases at about 150 °C, as do the activation energies of all LICVD samples (e.g., see Fig. 1).

IV. THEORY OF METASTABLE CONDUCTIVITY CHANGES

A. Defect relaxation

In this section we present a simple model of the thermodynamics and kinetics of the metastable conductivity changes observed in heavily doped n-type a-Si:H. From our results, as from those of Ast and Brodsky[1] and Street *et al.*,[4] it is evident that rapid quenching freezes a particular nonequilibrium structure into the film below a transition temperature T^* which depends on cooling rate. Below T^*, the rate of equilibration is too slow to bring the structure to equilibrium on experimental time scales. Above T^*, the structure has time to reach equilibrium and the conductivity is independent of the annealing time or the cooling rate. We assume that the defects that control the Fermi energy, E_F, equilibrate via a two-level system of structural configurations as sketched in Fig. 4. There is a high-energy "defect" configuration separated by an energy barrier from a lower-energy "normal" configuration. The barrier, E_b, kinetically retards equilibration below T^*, leaving an overpopulation of defect states after quenching. After an anneal at temperature, T, long enough so that $T > T^*$, the number of defect states, $D(T)$, is determined by thermodynamics in the two-level system. Bar-Yam *et al.*[9] have analyzed the dependence of T^* upon cooling rate and annealing time for such a two-level system and their results are in qualitative agreement with our experiments.

To move E_F, the electronic energy levels associated with the defect configuration must be different from those of the normal configuration. If, for example, the defect configuration yields an occupied electronic energy level *above* E_F, and the normal configuration yields a level *below* E_F, then creation of the defect configuration induces an increase in E_F. We now use this model to analyze the isothermal relaxation experiment.

We assume that the defects reach their equilibrium density, $D(T_r)$, if the material is held at T_r for sufficiently long times. Quenching results in the formation of $D(T^*)$ defects, where T^* is the freezing-in temperature. If the quench is fast, $T^* > T_r$ and $D(T^*) > D(T_r)$. When the temperature is abruptly raised to T_r there must be $\delta D_0 = D(T^*) - D(T_r)$ excess metastable defects in the film. This means that δD_0 electronic states that would have been below E_F at equilibrium are frozen-in above E_F in the metastable

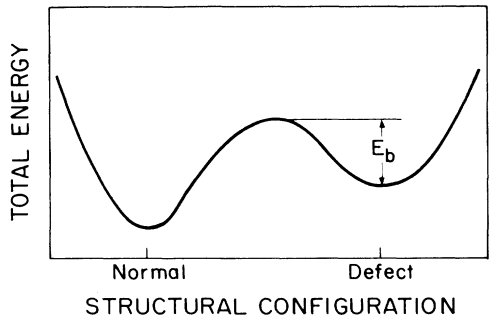

FIG. 4. Schematic diagram of the two-level system controlling the metastable conductivity changes. A barrier energy, E_b, retards reequilibration of excess defects.

quenched state at T_r. In the isothermal relaxation experiment, the electronic distribution comes to immediate thermal equilibrium when the temperature is increased to T_r, but the excess defect population at T_r, $\delta D(t)$, relaxes slowly toward equilibrium. If the defect relaxation time is τ, then

$$\delta D(t)=\delta D_0 \exp(-t/\tau) ,$$

and the number of excess defects that have relaxed to the normal configuration, i.e., the number of filled electronic states that have moved from above to below E_F is

$$N(t)=\delta D_0[1-(e^{-t/\tau})] . \quad (1)$$

We now use Eq. (1) to predict the form of the conductivity decay in an isothermal relaxation experiment, assuming two different densities of electronic states near E_F.

B. Constant density of states

The Fermi energy of n-type samples is most likely located in an exponentially decaying region of the density of states

$$g(E)=g_c \exp[-(E_c-E)/kT_c] , \quad (2)$$

where $T_c=310$ K (Ref. 14) and g_c is the density of states at the conduction-band mobility edge, E_c. The quenched and slow-cooled Fermi energy positions, E_F^Q and E_F^{SC}, are separated by only about 0.02 eV, corresponding to a change in $g(E)$ of about a factor of 2. We therefore initially assume that the density of states is essentially constant between E_F^Q and E_F^{SC}, given by $g(E)\equiv g$. In Sec. IV C we extend the analysis to an exponential density of states.

Initially, E_F is E_F^Q and the activation energy is E_a^Q. At $t=0$, the temperature is increased to T_r and as time passes, E_F moves deeper into the gap due to the relaxation process. At time, t, $E_F(t)=E_F^Q+\Delta E_F(t)$, where

$$\Delta E_F(t)=\frac{-N(t)}{g}=-\delta D_0[1-\exp(-t/\tau)]/g$$

from Eq. (1).

We assume that the conductivity preexponential, σ_0, is essentially constant during the relaxation process, so that

$$\sigma(t)=\sigma_0 \exp\{-[E_C-E_F(t)]/kT_r\} . \quad (3)$$

The ratio of $\sigma(t)$ to its final value is then

$$\frac{\sigma(t)}{\sigma_f}=\frac{\sigma_0 \exp[E_a^Q+\Delta E_F(t)]/kT_r}{\sigma_0 \exp[E_a^Q-\delta D_0/g]/kT_r}$$

$$=\exp[(\delta D_0/gkT_r)\exp(-t/\tau)] . \quad (4)$$

Equation (4) can be rewritten as

$$\log_{10}\left[\log_{10}\frac{\sigma(t)}{\sigma_f}\right]=\log_{10}\left[\frac{\delta D_0}{2.3gkT_r}\right]-t/2.3\tau , \quad (5)$$

and a fit of our isothermal annealing data to this function is described in Sec. V.

C. Exponential density of states

In this section we use the exponential band-tail of Eq. (2) to obtain an alternative expression for the current decay during isothermal relaxation. In this case the relaxation of excess defects moves E_F according to

$$N(t)=\int_{E_a^Q}^{E_a^Q+\Delta E_F(t)} g(E)dE$$

$$=g_0 kT_c\{1-\exp[-\Delta E_F(t)/kT_c]\} , \quad (6)$$

where we have defined $g_0=g_c \exp(-E_a^Q/kT_c)$, the density of states at E_F at $t=0$. Solving Eq. (6) for $\Delta E_F(t)$ and substituting the corresponding value of $E_F(t)$ into the expression of Eq. (3) for $\sigma(t)$, we find

$$\frac{\sigma(t)}{\sigma_i}=\frac{\sigma_0 \exp(\{-E_a^Q+kT_c \ln[1-N(t)/g_0 kT_c]\}/kT_r)}{\sigma_0 \exp(-E_a^Q/kT_r)}$$

$$=\exp\{(1/\alpha)\ln[1-N(t)/g_0 kT_c]\} ,$$

where $\alpha\equiv T_r/T_c$.

Substituting $N(t)$ from Eq. (1), we obtain a simple expression for $\sigma(t)$:

$$1-\frac{g_0 kT_c}{\delta D_0}\left[1-\left[\frac{\sigma(t)}{\sigma_i}\right]^{\alpha}\right]=\exp(-t/\tau) . \quad (7)$$

In principle, the parameter $g_0 kT_c/\delta D_0$ can be obtained by experimentally determining the value of $\Delta E_F(\infty)$ and substituting it into Eq. (6).

V. DISCUSSION

Our conductivity measurements on heavily P-doped LICVD a-Si:H yield results qualitatively similar to those previously reported for P-doped glow-discharge a-Si:H.[1,2] Structural changes are quenched into the film and these result in conductivity changes that can be attributed primarily to a shift of E_F.[1] The magnitude of this shift depends on T^*, the freezing-in temperature of the defect population, with T^* determined by cooling

rate. During slow heating, the defect population unfreezes and returns to equilibration at a different temperature, T_E. Annealing significantly below T^* leaves the low-temperature conductivity unaffected. The value of T_E should increase with increasing heating rate, but should not depend strongly upon the value of T^* frozen-in during quenching. Although previous work[3] used a heating rate of 3 °C/min during the slow heating, we used values in the range of 0.5 °C–1.0 °C/min. Despite this slower rate of heating, we obtain $T_E = 240$–280 °C for several sets of experiments on heavily P-doped material, much larger than the previously determined $T_E = 140$ °C.[3] Thus we conclude that the metastable defects quenched into LICVD a-Si:H have a larger barrier to reequilibration or a slower rate constant for annealing than those quenched into glow-discharge a-Si-H. We subsequently estimate the magnitude of this barrier for LICVD films from the results of the isothermal relaxation experiments. It should be noted, however, that while T_E was found to be about 30% higher in LICVD than in glow-discharge a-Si:H, the deposition temperature of the LICVD films was 400 °C, also about 30% higher than the glow-discharge films.

The B-doped LICVD film also exhibits a higher T_E than B-doped glow-discharge films, 185 °C compared to 95 °C. However, the curves of Fig. 3 indicate that even above 185 °C, there remain quenched-in defects that are unequilibrated. The simplest explanation of this result is that the conductivity difference above 185 °C is caused by a second defect with a value of T^* for these annealing times that is higher than T_a. Storage at room temperature for one month, followed by another 285 °C anneal at T_a caused this second defect to completely relax, resulting in a measurement of $\sigma^{SC}(T)$ identical to the first. Thus multiple defects are indeed present in this film, each having a different value of T^* and/or different annealing kinetics.

Although slow-heating conductivities differ from run-to-run in undoped LICVD a-Si:H, neither repeatable changes due to quenching nor a definite T_E are observed. In intrinsic films, E_F lies in a region of low density of states, making these films more susceptible to changes in surface adsorbates,[15] and this may be controlling the conductivity even though σ is measured under vacuum conditions. Of course, it is precisely the fact that E_F is unpinned in intrinsic films which should make the conductivity very sensitive to small concentrations of electronic states shifting from below to above E_F. However, we observed no dramatic changes that can be attributed to the quenching rate. Thus it is likely that either the dopant atom itself is involved in the metastable defect observed in doped films or that the metastable changes in $g(E)$ do not shift states in the midgap region, so that the conductivity is unaffected. Evidence for metastable changes in undoped a-Si:H reported by Smith *et al.*[6] support the latter hypothesis, as does our failure to observe a definite T_E in the lightly P-doped sample ($E_F \approx E_c - 0.5$ eV), in spite of the presence of P. In this case, P is present, yet metastable conductivity changes are not observed.

Figure 5 shows a plot of $\log_{10}[\log_{10}(\sigma(t)/\sigma_f)]$ for the isothermal relaxation at $T_r = 200$ °C in order to demonstrate the fit to the theoretical expression of Eq. (5). According to theory, the slope of the line is inversely proportional to the relaxation time, τ, at T_r. At $T_r = 200$ °C, a fast decay dominates the first 3 h of the experiment, but it gives way to a slower decay with $\tau = 8.4$ h lasting nearly 24 h. These two linear regimes are observed for all $T_r \leq 240$ °C. Above 260 °C, the fast decay is not observed, most likely because it is obscured by the 10–20 min required for the film temperature to equilibrate with the heated block and reach T_r. While the fast decay may be associated with the annealing of a second metastable defect, we note that this decay rate is observed from σ_{max} down to the extrapolated value of $\sigma^Q(T_r)$ that was determined from the low-temperature data. It may therefore be caused instead by another phenomenon related to the curvature of the Arrhenius plots. In any case, we ignore the transient effect and focus on the kinetics implied by the slower decay observed for longer times.

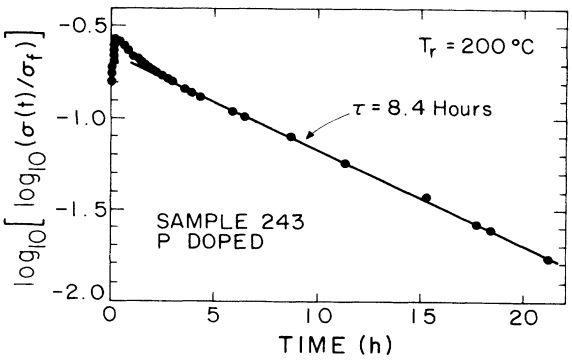

FIG. 5. Log_{10} of $\log_{10}$ electrical conductivity of quenched sample 243 during isothermal annealing at 200 °C.

Estimates of the number of excess defects, δD_0, can be obtained from the intercept of curves similar to that of Fig. 5, in accordance with Eq. (5). Taking[16] $g_c = 5 \times 10^{21}/\text{cm}^3$, and using Eq. (2), we find δD_0 is of the order of 10^{17} cm^{-3}.

In Fig. 6 we plot $1/\tau(T_r)$ for each isothermal relaxation as a function of $1/T_r$. We find $1/\tau = \nu_0 \exp(-E_b/kT_r)$ fits all data except the lowest temperature ($T_r = 170$ °C) point. It is reasonable to assume that τ (170 °C) is shortened by secondary annealing mechanisms that compete with the dominant higher-temperature defect annealing mechanism. A least-squares fit to higher-temperature data yields $E_b = 1.1$ eV and $\nu_0 = 2 \times 10^7$/sec. The value of the barrier energy is similar to that observed during annealing of light-induced metastable defects in a-Si:H[17] We think that the low value of ν_0 is due to a microscopic process involving annealing of defects that must first diffuse toward one another.

We have also fit the isothermal relaxation data to Eq. (7), which is applicable to the case of an exponential density of states, and we obtained similar values of τ at each T_r. To obtain a linear fit, however, we had to adjust the

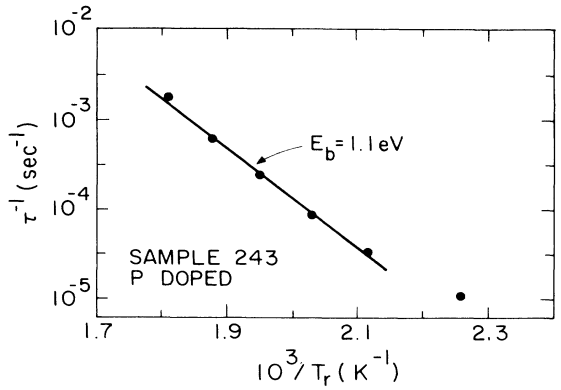

FIG. 6. Inverse relaxation time vs inverse relaxation temperature for isothermal relaxations of quenched sample 243. Solid line is a fit to all but the lowest temperature point.

free parameter $g_0 kT_c/\delta D_0$. We therefore prefer fitting to the parameter-free expression derived for an essentially constant density of states.

Ast and Brodsky[1] analyzed their isothermal relaxation data by assuming second-order reaction kinetics and a linear relationship between the number of microscopic processes and the excess conductivity. We attempted the same fit, but found that our model based on first-order reaction kinetics gives a better fit to the experimental data. In view of the small number of defects involved in these metastable changes, and without compelling evidence for interaction between defects, we feel that second-order kinetics that require reactions between defects are unlikely.

Finally, we speculate about possible microscopic origins of the metastable defect in P-doped *a*-Si:H. Street *et al.*[4] proposed several defect reactions and suggested that these are mediated by hydrogen, which exists in a submatrix that undergoes a glass transition at T^*. We focus instead on the underlying defect reactions and use the notation of Adler[18] to describe them. The most likely mechanism for an increased E_F in the doped films is an increase in active dopant concentrations. From thermodynamic considerations, a higher concentration of P_4 centers is expected at higher temperatures for $T > T^*$,[9] and if some of these are quenched in, they clearly increase E_F by transferring the highest-energy electron on the phosphorus atom to a weak antibonding (T_4^-) or other level at E_F. A mechanism for the annealing, which decreases E_F, can be represented as

$$P_4^+ + T_4^- \rightarrow P_3^0 + T_3^- \ . \tag{8}$$

Since the concentration of available sites is [P], the number of P_4^+ centers would be small in lightly doped *a*-Si:H and zero is undoped *a*-Si:H. This could explain our failure to observe the metastable defect in the lightly doped and undoped films. The increase of E_F upon quenching induced by creation of P_4^+ sites also explains the sweep-out data[4] when the theory of the experiment is worked out in detail.[19] This reaction, however, cannot explain the increase in subgap optical absorption observed in quenched *undoped* *a*-Si:H by Smith *et al.*,[6] which requires participation of an intrinsic defect.

VI. CONCLUSIONS

We have measured the electrical conductivity of several LICVD *a*-Si:H films, undoped, *p*-type, and *n*-type, as a function of different thermal annealing and quenching cycles. On the basis of the results obtained, we proposed a model relating the observed shifts of E_F to defects formed at high temperature via equilibration and then frozen-in below a temperature T^* that depends on the cooling rate. We find that first-order kinetics apply to the defect annealing, and the theory can be used to set the barrier that retards equilibration at approximately 1.1 eV. We estimate that 10^{17} cm^{-3} excess defects are quenched-in and cause the observed conductivity changes in *n*-type films. The equilibration temperature upon slow heating, T_E, was found to be considerably higher in LICVD films than in plasma-deposited films. In *p*-type samples, there is evidence for a second defect with a higher value of T^*. No similar metastable conductivity changes are evident in intrinsic or lightly P-doped samples, most likely because creation of metastable defects do not shift states across the region 0.5 to 0.9 eV below E_c. A microscopic model for the metastable defect annealing reaction was discussed.

ACKNOWLEDGMENT

This research was supported, in part, by the Solar Energy Research Institute under Contract No. XL-4-03032.

*Present address: Solar Energy Research Institute, 1617 Cole Boulevard, Golden, CO 80401.
†Deceased.

[1] D. G. Ast and M. H. Brodsky, *Physics of Semiconductors 1978*, Institute of Physics Conference Series No. 434, edited by B. L. H. Wilson (IOP, London, England, 1979), p. 1159.
[2] R. A. Street, J. Kakalios, and T. M. Hayes, Phys. Rev. B **34**, 3030 (1986).
[3] J. Kakalios and R. A. Street, Phys. Rev. B **34**, 6014 (1986).
[4] R. A. Street, J. Kakalios, C. C. Tsai, and T. M. Hayes, Phys. Rev. B **35**, 1316 (1987).
[5] R. A. Street and J. Kakalios, Philos, Mag. B **54**, L21 (1986).
[6] Z E. Smith, S. Aljishi, D. Slobodin, V. Chu S. Wagner, P. M. Lenahan, R. R. Arya, and M. S. Bennett, Phys. Rev. Lett. **57**, 2450 (1986).
[7] R. Bilenchi, I. Gianinoni, and M. Musci, J. Appl. Phys. **53**, 6479 (1982).
[8] M. Meunier, T. R. Gattuso, D. Adler, and J. S. Haggerty, Appl. Phys Lett. **43**, 273 (1983).
[9] Y. Bar-Yam, D. Adler, and J. D. Joannopoulos, *Stability of Amorphous Silicon Alloy Materials and Devices*, AIP Conf. Proc. No. 157, edited by B. L. Stafford and E. Sabisky (AIP, New York, 1987), p. 185.
[10] M. Meunier, J. H. Flint, J. S. Haggerty, and D. Adler, J.

Appl. Phys. **62**, 2812 (1987).
[11]M. Meunier, J. H. Flint, J. S. Haggerty, and D. Adler, J. Appl. Phys. **62**, 2822 (1987).
[12]H. M. Branz, S. Fan, J. H. Flint, B. T. Fiske, D. Adler, and J. S. Haggerty, Appl. Phys. Lett. **48**, 171 (1986).
[13]H. M. Branz, Ph.D. thesis, MIT, 1987.
[14]T. Tiedje, *Semiconductors and Semimetals,* edited by J. I. Pankore (Academic, New York, 1984), Vol. 21C, p. 207.
[15]M. Tanielian, Philos. Mag. B **45**, 435 (1982).
[16]W. B. Jackson, S. M. Kelso, C. C. Tsai, J. W. Allen, and S.-J. Oh, Phys. Rev. B **31**, 5187 (1985).
[17]M. Stutzmann, W. B. Jackson, and C. C. Tsai, Phys. Rev. B **32**, 23 (1985).
[18]D. Adler, J. Non-Cryst. Solids **35-36**, 819 (1980).
[19]H. M. Branz, M. Silver, and D. Adler, Philos. Mag. (to be published).